

Lawrence Berkeley National Laboratory

Recent Work

Title

ANALYSIS OF TRANSPORT PROCESSES IN VERTICAL CYLINDER EPITAXY REACTORS

Permalink

<https://escholarship.org/uc/item/6pw1d5kd>

Author

Manke, C.W.

Publication Date

1976-06-01

Submitted to Journal of the Electrochemical
Society

LBL-5187
Preprint C. |

ANALYSIS OF TRANSPORT PROCESSES IN VERTICAL
CYLINDER EPITAXY REACTORS

C. W. Manke and L. F. Donaghey

RECEIVED
LAWRENCE
BERKELEY LABORATORY

JUL 26 1976

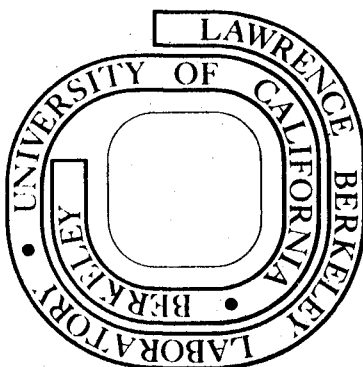
June 1976

LIBRARY AND
DOCUMENTS SECTION

Prepared for the U. S. Energy Research and
Development Administration under Contract W-7405-ENG-48

For Reference

Not to be taken from this room



LBL-5187
C. |

DISCLAIMER

This document was prepared as an account of work sponsored by the United States Government. While this document is believed to contain correct information, neither the United States Government nor any agency thereof, nor the Regents of the University of California, nor any of their employees, makes any warranty, express or implied, or assumes any legal responsibility for the accuracy, completeness, or usefulness of any information, apparatus, product, or process disclosed, or represents that its use would not infringe privately owned rights. Reference herein to any specific commercial product, process, or service by its trade name, trademark, manufacturer, or otherwise, does not necessarily constitute or imply its endorsement, recommendation, or favoring by the United States Government or any agency thereof, or the Regents of the University of California. The views and opinions of authors expressed herein do not necessarily state or reflect those of the United States Government or any agency thereof or the Regents of the University of California.

Analysis of Transport Processes in Vertical
Cylinder Epitaxy Reactors*

C. W. Manke and L. F. Donaghey

Materials and Molecular Research Divison, Lawrence Berkeley Laboratory
and Department of Chemical Engineering, University of California,
Berkeley, California 94720

June, 1976

Abstract

Momentum, heat and mass transfer processes were studied in a vertical cylinder reactor for the epitaxial growth of Si from SiCl_4 in H_2 by chemical vapor deposition. An analytical solution to the problem of heat and mass transfer in a tapered annulus is presented based on constant transport properties and fully-developed laminar flow. The mean gas-phase temperature and deposition rate distribution of silicon are calculated within the reactor using the developing temperature model. Results of experimental studies of silicon deposition from SiCl_4 in H_2 at 1200°C in a vertical cylinder reactor are compared with the analytical results, and with other models of diffusion-controlled chemical vapor deposition. This study provides an analytical basis for epitaxial deposition rate distributions in vertical cylinder reactors, and for reactor design to improve the yield and uniformity of epitaxial growth.

* This report was done with support from the United States Energy Research and Development Administration. Any conclusions or opinions expressed in this report represent solely those of the authors and not necessarily those of The Regents of the University of California, the Lawrence Berkeley Laboratory or the United States Energy Research and Development Administration.

I. ANALYSIS OF TRANSPORT PROCESSES IN A VERTICAL CYLINDER REACTOR

INTRODUCTION

Vertical cylinder (barrel) reactors have been developed recently for the epitaxial growth of semiconductor layers by chemical vapor deposition. This type of reactor has already demonstrated the potential for scale-up of the epitaxial growth process. The increased through-put of the vertical cylinder reactor as compared to the horizontal reactor is particularly important in the semiconductor industry where high volumes of silicon bipolar devices are involved.

Growth rate uniformity of epitaxial silicon by chemical vapor deposition is of great importance for semiconductor applications. The yield of finished devices is sharply diminished by non-uniformity of the thickness of the epitaxial silicon layer either on the individual wafers or from wafer to wafer within the processing batch. Growth rate uniformity, of course, must be accomplished using an economical quantity of reactant gas. Successful processing, therefore, requires the development of reactor design principles for achieving optimum growth rate uniformity at reasonable reactant flow rates. The development of mathematical models for the description of transport processes and the deposition rate distribution of silicon in the vertical cylinder reactor is examined in this paper.

Models for the chemical vapor deposition rate of silicon have been studied by a number of investigators. Eversteijn and coworkers(1,2) and Rundle (3,4) have developed models for the growth rate of silicon in horizontal reactors by considering diffusion through a laminar sublayer adjacent to a turbulent flow region. Fujii et al. (5)

developed a quantitative model of silicon deposition rates in vertical cylinder reactors, and quantitative studies were reported by Dittman (6).

In the above works, the gas temperature profile was considered to be constant over the entire length of the reactor. In a real reactor, however, the temperature, velocity and concentration profiles can be expected to change rapidly in the entrance region near the leading edge of the constant-temperature susceptor before achieving the constant, or fully developed distributions assumed by the above models.

Several of the above models recognize the need for incorporating boundary layer theory into a growth rate model. For example, Eversteijn assumes a boundary layer thickness equal to a fraction of the channel width, and Dittman used a modified form of the Chilton-Colburn analogy to obtain properties of boundary layer flow over a flat plate. Unfortunately, the geometry and transport phenomena of the vertical cylinder reactor are not well described by either of these models. It will be shown in this paper that mass transfer analogies based on turbulent flow over a flat plate do not give a satisfactory prediction of the silicon growth rate in the vertical cylinder reactor, and that what is needed is a method for predicting the growth rate based on the theory of transport in the laminar, developing flow regime, the Graetz problem in an annular passage.

Important theoretical methods for assessing transport in a fluid in fully developed laminar flow can be found in the fluid mechanical literature. Graetz (7) solved the problem of developing

heat transfer in tube by means of an eigenfunction expansion, and Nusselt (8) improved the accuracy of his calculation of the first three eigenvalues. Brown (9) solved the Graetz problem in a flat duct, and the extension to a right circular annulus has been studied by Hatton and Quarmby (10), and by Reynolds and co-workers (11,12).

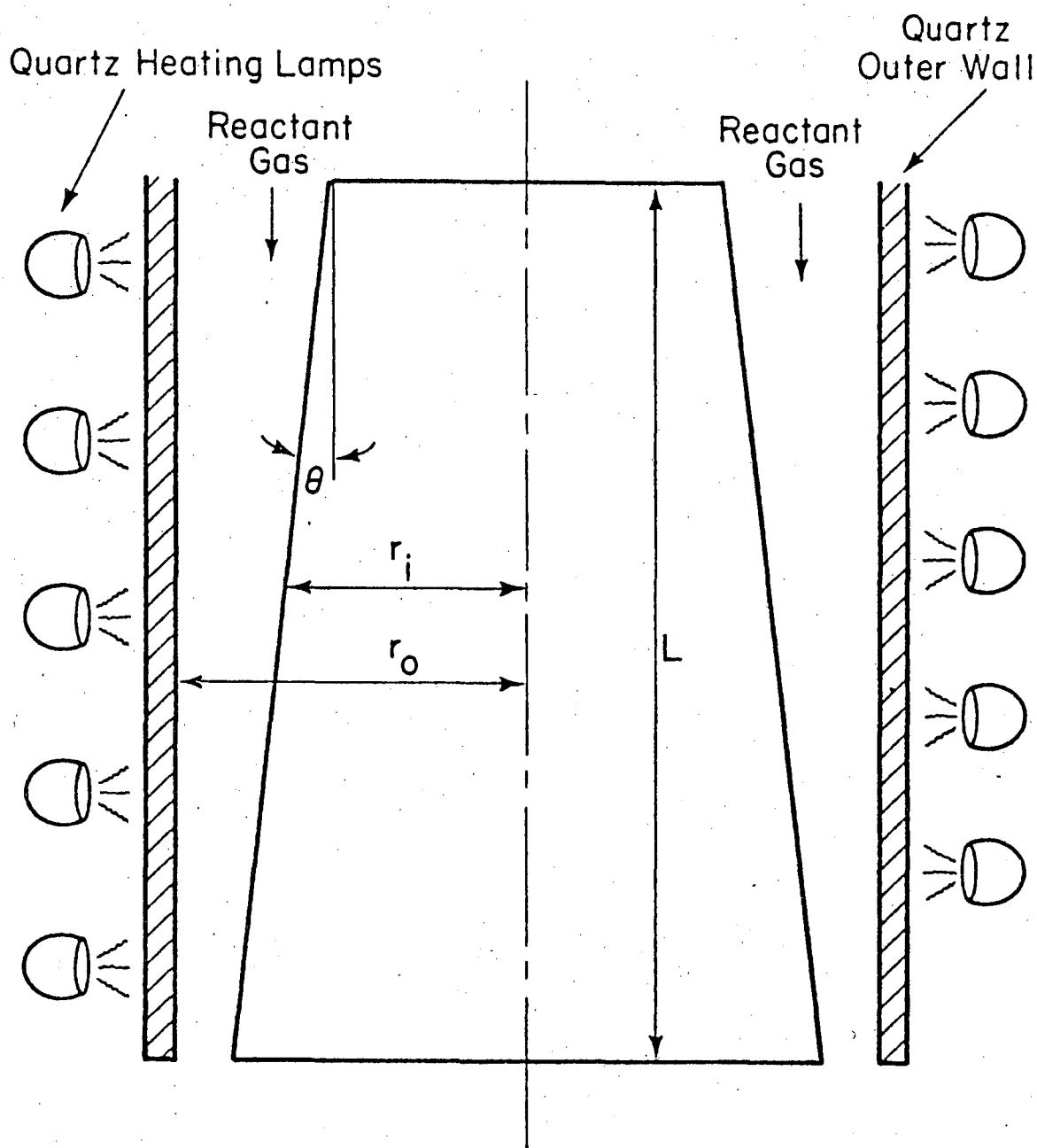
In this paper, a solution to the Graetz problem of heat transfer in an annular passage will be used to demonstrate that the temperature profile in the vertical cylinder reactor develops over a significant portion of the susceptor length; the mean temperature of the gas increases with downstream position until the fully developed value is attained. Mass transfer will be shown to have a positive temperature dependence resulting in enhancement of the growth rate as temperature increases. Finally, a method for calculating the growth rate will be presented which accounts for the effects of developing flow in the annular passage. This method, based on the results of an extensive analysis of heat transfer in annular passages is used to study the effects of gas flow rate and susceptor tilt angle on growth rate uniformity and reactant yield. Finally, growth rate calculations are compared to those predicted by other published models and to experimental results obtained in a commercial vertical cylinder reactor.

THEORY

The Vertical Cylinder Reactor

For silicon epitaxial growth from SiCl_4 , a dilute mixture of SiCl_4 in hydrogen is passed through an annular passage between a cylindrical outer quartz wall of the reactor and an octagonal silicon carbide-coated, graphite susceptor, idealized here as the frustum of a cone or as a right-circular cylinder. The vertical cylinder reactor is shown schematically in Fig.1.

In practice, silicon substrate wafers are placed on the faces of the susceptor which is radiantly heated by quartz lamps during operation, with forced air used to cool the lamps and the outer wall of the reactor. Typical operating conditions for silicon epitaxial growth from SiCl_4 are a susceptor temperature near 1200°C , a gas mixture containing about one percent SiCl_4 in hydrogen, and a flow rate yielding Reynolds numbers near 100. Under those conditions the fluid is in laminar flow. Shaw(13) reports that the temperature at which mass transfer control of the growth rate predominates over kinetic control is not precisely known; however, several experimental studies indicate that deposition of epitaxial silicon from a dilute SiCl_4 reactant is entirely diffusion controlled at 1200°C . The silicon deposition reaction is surface-catalyzed and therefore occurs only at the surface of the heated susceptor. Silicon deposition occurs on all parts of the susceptor surface. Calculation of the growth rate, then, is a matter of determining the rate of mass transfer of the reactant from the gas stream to the susceptor surface. Since the mass transfer rate is dependent on the velocity and temperature



XBL 764-949

FIGURE 1.

THE VERTICAL CYLINDER REACTOR

distributions in the gas phase, equations governing all three transport phenomena must be solved.

Transport Equations

The steady state equations governing transport are:

- 1) The momentum equation in the axial direction:

$$\rho v_r \frac{\partial v_z}{\partial r} + v_z \frac{\partial v_z}{\partial z} = - \frac{\partial p}{\partial z} + \rho g_z + \mu \frac{1}{r} \frac{\partial}{\partial r} \left(r \frac{\partial v_z}{\partial r} \right) \quad (1)$$

- 2) The energy equation in the axial direction:

$$v_r \frac{\partial T}{\partial r} + v_z \frac{\partial T}{\partial z} = \alpha \frac{1}{r} \frac{\partial}{\partial r} \left(r \frac{\partial T}{\partial r} \right) \quad (2)$$

- 3) The equation for continuity of the diffusing species, axial direction:

$$v_r \frac{\partial X}{\partial r} + v_z \frac{\partial X}{\partial z} = D_{12} \frac{1}{r} \frac{\partial}{\partial r} \left(r \frac{\partial X}{\partial r} \right) \quad (3)$$

- 4) The equation of continuity:

$$\frac{1}{r} \frac{\partial}{\partial r} (\rho r v_r) + \frac{\partial}{\partial z} (\rho v_z) = 0 \quad (4)$$

The fluid physical properties in the above equations, μ , ρ , α , D_{12} are assumed to be constant, a necessary condition for a simplified analytical treatment.

The radial velocity distribution for fully developed laminar flow

is the solution to Eq. (1). In a cylindrical annulus the solution has the form,

$$U(r) = \frac{2U_m}{M}(1 - \bar{r}^2 + B \ln \bar{r}) \quad (5)$$

where M and B are constants. The buoyancy term, g_z , of Eq.(1) is neglected in deriving Eq.(5); this assumption leads to an error at the susceptor leading edge where a large thermal gradient is present, but the omission of the buoyancy term is a simplification necessary for analytical treatment. The condition of stable, fully developed laminar flow in the reactor is the basis for the following mathematical description of transport processes.

The following dimensionless parameters are useful in reducing the transport equations to simple forms:

$$\bar{r} = r/r_o$$

$$\theta(\bar{x}) = \frac{T - T_i}{T_e - T_i}, \quad \bar{x} = \frac{z}{\text{RePrd}_h} \quad (6)$$

$$X(\bar{z}) = \frac{X - X_i}{X_e - X_i}, \quad \bar{z} = \frac{z}{\text{ReScd}_h}$$

In addition, it is useful to define the bulk-mean reduced temperature and reactant mole fraction as follows;

$$\begin{aligned}\theta_m &= (A U_m)^{-1} \int_A U \theta \, dA \\ X_m &= (A U_m)^{-1} \int_A U X \, dA\end{aligned}\tag{7}$$

where the integral is over the area of the annulus at a given axial position.

For fully developed velocity, the energy equation, Eq. (2), can be reduced to the dimensionless temperature equation which follows. Using the dimensionless mole fraction above, the reactant mass continuity equation can be reduced to a similar form:

$$\frac{\partial^2 \theta}{\partial \bar{r}^2} + \frac{1}{\bar{r}} \frac{\partial \theta}{\partial \bar{r}} = \frac{U(\bar{r})}{\alpha} \frac{\partial \theta}{\partial \bar{x}}\tag{8}$$

$$\frac{\partial^2 X}{\partial \bar{r}^2} + \frac{1}{\bar{r}} \frac{\partial X}{\partial \bar{r}} = \frac{U(\bar{r})}{D_{12}} \frac{\partial X}{\partial \bar{z}}\tag{9}$$

The boundary value problems for solving Eqs (8) and (9) can be made homogeneous by subtracting the fully developed solutions which are valid as \bar{x} and \bar{z} tend to infinity. The complete solutions to Eqs (8) and (9) can then be solved by separation of variables in the form:

$$\theta = \theta_{fd} + \sum_{n=0}^{\infty} C_n F_n \exp(-\lambda_n \bar{x})\tag{10}$$

where the functions F_n satisfy a differential equation of the Sturm-

Liouville type.

Solution of the transport equations for developing flow is a difficult problem. Reynolds, McCuen, and Lundberg (11,12), however, have obtained solutions for the coefficients C_n by numerical integration using an iterative method developed by Berry and de Prima (14). As a result of their work, θ_m and the Nusselt number, Nu , (and by analogy X_m and Sh for mass transfer) are given for several types of boundary conditions in an annular passage. These functions will be used in a differential material balance expression to calculate the growth rate of silicon in the vertical cylinder reactor, taking into account the effects of developing heat and mass transfer in a fully developed velocity distribution.

Boundary Conditions and Initial Values

Heat Transfer

Heating of the susceptor in the vertical cylinder reactor is typically achieved with high-intensity quartz-iodide lamps, which hold the entire susceptor at a constant temperature. The outer wall is air-cooled but subject to radiant heating from the hot susceptor and from the quartz lamps as well as to convective heating both inside and outside the reactor. As a result the boundary condition at this wall is quite difficult to determine. Experimental measurements of the outer wall temperature indicate that the quartz wall reaches a temperature near 773°K over the major portion of the wall (15). Therefore the temperature boundary condition can be approximated by assuming the entire outer wall to be at a constant temperature of 773°K .

Thus,

$$T = \begin{cases} 1473^\circ\text{K}, & r = r_i, 0 < z \\ 773^\circ\text{K}, & r = r_o, 0 < z \end{cases} \quad (11)$$

$$(12)$$

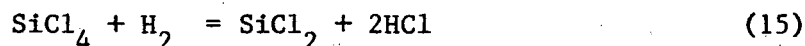
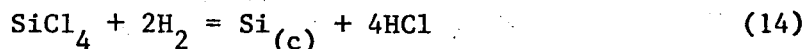
Since the gas enters the reactor at room temperature, the initial value is taken as 298°K .

For the boundary conditions of specified temperatures at both walls of the annulus, the mean temperature of the gas at a downstream location is determined from dimensionless temperature functions according to the following equation:

$$T_m(x) = \theta_{mi}(\bar{x}) \cdot (T_i - T_e) + \theta_{mo}(\bar{x}) \cdot (T_o - T_e) + T_e \quad (13)$$

Mass Transfer

The boundary condition for mass transfer at the susceptor surface is specified by chemical reaction equilibria at the temperature of the susceptor, since for susceptor temperatures near 1473°K the growth rate is limited by diffusion rather than by the kinetics of the surface reactions. The deposition reaction equilibria are primarily:



Sirtl, Hunt, and Sawyer (16) indicate that a very low partial pressure of SiCl_4 ($\sim 10^{-5}$) exists in the equilibrium composition at 1473°K for the Si-H-Cl system at low values of the Cl/H ratio (0.02327 for 1.15% SiCl_4 in H_2). Since the driving force for diffusion of the reactant to the

susceptor surface is the difference between the partial pressure in the bulk gas stream ($\sim 10^{-2}$) and the partial pressure at the susceptor surface ($\sim 10^{-5}$), the boundary condition for mass transfer at the inner surface can be approximated very well by taking the reactant concentration to be zero. Since deposition does not occur at the outer wall, a flux equal to zero is specified. The boundary conditions for mass transfer are then:

$$X = 0, \quad r = r_1, \quad z > 0 \quad (16)$$

$$\frac{dX}{dr} = 0, \quad r = r_0, \quad z > 0 \quad (17)$$

For an inlet gas containing 1.15% (vol.) SiCl_4 , the initial condition is:

$$X = .0115 \text{ at } z = 0 \text{ and } r_1 \leq r \leq r_0 \quad (18)$$

Thermodynamic Yield From Reactant Gas

While Eq.(14) is the overall reaction for silicon deposition, the gas species SiCl_2 will also be formed in an equilibrium mixture by the competing side reaction given in Eq.(15). The yield of epitaxial silicon produced from the reactant diffusing to the susceptor will be reduced if SiCl_2 is formed in significant quantities. Sirtl et al. report the equilibrium yield of solid silicon from SiCl_4 as a function of the SiCl_4 mole fraction. For a SiCl_4 mole fraction of .0115 and a temperature of 1400 °K, the yield of silicon is approximately seventy percent.¹⁾ To account for the reduction in deposition efficiency caused by the side reaction forming SiCl_2 , the flux of SiCl_4 to the susceptor surface must be multiplied by a deposition efficiency, η ,

1) Determined from Fig. 3b of reference 16.

to obtain the yield of deposited silicon from the reactant gas. Since reaction kinetics are assumed to be very fast at the temperature of the susceptor, 1473 °K, the deposition efficiency used in this study is the equilibrium yield for a SiCl_4 mole fraction of .0115, which is 0.7.

Growth Rate Equation

The growth rate can be calculated directly from the dimensionless flux of reactant for a given value of the Sherwood number. The dependence of the growth rate on axial distance can be easily developed by taking a material balance on a differential ring element of the reactor annulus. The molar flow rates of reactant entering and leaving the element are $\dot{M} \bar{X}|_z$ and $\dot{M} \bar{X}|_{z+\Delta z}$, respectively. The molar reaction rate within the element is then:

$$2\pi r_i \Delta z \text{ Sh } \frac{D_{12}}{d_h} (\bar{X} - X_i) P/(R T_m) \quad (19)$$

where $X_i = 0$. By balancing the above rates one obtains the differential equation for the reactant concentration:

$$-\dot{M} \frac{d\bar{X}}{dz} = \frac{P 2\pi r_i \text{ Sh } D_{12}}{d_h R T_m} \bar{X} \quad (20)$$

After integration this equation becomes:

$$\bar{X} = X_o \exp \left\{ - \frac{2\pi P}{M R} \int_0^z \frac{r_i \text{Sh } D_{12}}{d_h T_m} dz \right\} \quad (21)$$

The flux to the surface is then given by

$$\frac{P}{R T_m} D_{12} \left. \frac{d\bar{X}}{dr} \right|_{r=r_i} = \frac{P}{R T_m} \text{Sh } \frac{D_{12}}{d_h} (\bar{X} - X_i) \quad (22)$$

From Eqs (21) and (22) and the deposition efficiency, η , the linear growth rate expression becomes:

$$G = \eta \cdot 6 \times 10^5 \frac{M_{Si}}{P_{Si}} \frac{P \text{Sh } D_{12}}{R T_m d_h} X_o \exp \left\{ - \frac{2\pi P}{M R} \int_0^z \frac{r_i \text{Sh } D_{12}}{d_h T_m} dz \right\} \quad (23)$$

Transport Properties

Transport properties are evaluated for the composition of the inlet gas containing 1.15% SiCl_4 and 98.85% H_2 on a molar basis. For heat transfer, the viscosity, density, thermal conductivity and heat capacity of the above mixture are evaluated at 298 °K. These properties are summarized in Table 1. An important result of the evaluation of properties for heat transfer is that the Prandtl Number for the mixture is 0.44 at 298 °K, much lower than the value of 0.7 usually used for gases. For the growth rate equation, properties were evaluated at average temperatures determined from the results of the heat transfer calculations. Viscosity, density, and the diffusion coefficient are given at different temperatures

in Table I.

Equations used to determine the values of transport properties were generally those recommended by Reid and Sherwood (17). A complete description of the evaluation of properties is given in Appendix II.

Temperature Dependence of the Growth Rate

The temperature dependence of the transport coefficients can be utilized to estimate the dependence of the growth rate on temperature. As explained in Appendix II, the diffusion coefficient is calculated by the equation:

$$D_{12} = 7.0861 \times 10^{-5} T^{3/2} / \Omega_0 . \quad (25)$$

The approximate temperature dependence of the diffusion coefficient in the temperature range of interest is $T^{1.674}$. If the effect of the exponential term of Eq. (21), the reactant depletion term, is neglected, the temperature dependence of the growth rate equation, Eq. (23), is $T^{0.674}$. The growth rate will therefore be enhanced as the temperature increases. A limit to this increase is established by thermodynamic conditions, however, since the amount of SiCl_2 in the vapor phase increases with temperature, causing the thermodynamic yield to reach a maximum at about 1430°K.

-15-

Table I

Transport coefficients for a reactant mixture
of 1.15% SiCl_4 - 98.85% H_2 .

<u>T, (°K)</u>	<u>μ_{mix}, (centipoise)</u>	<u>$\rho(\text{g/cm}^3)$</u>	<u>$D_{12}(\text{cm}^2/\text{a})$</u>	<u>Sc</u>
298	.00979	.0001511		
592	.01611	.00007606	1.162	1.823
726	.01870	.00006202	1.648	1.830
912	.02195	.00004937	2.426	1.833
997	0.2337	.00004516	2.818	1.836

Mol. Wt. of Mixture: 3.695

Thermal Conductivity of Mixture at 298°K: $9.20 \times 10^{-4} \frac{\text{cal}}{\text{cm sec}^\circ\text{K}}$

Heat Capacity of Mixture at 298°K: $7.039 \frac{\text{cal}}{\text{g-mole}^\circ\text{K}}$

Pr at 298°K: 0.44

RESULTS AND DISCUSSION

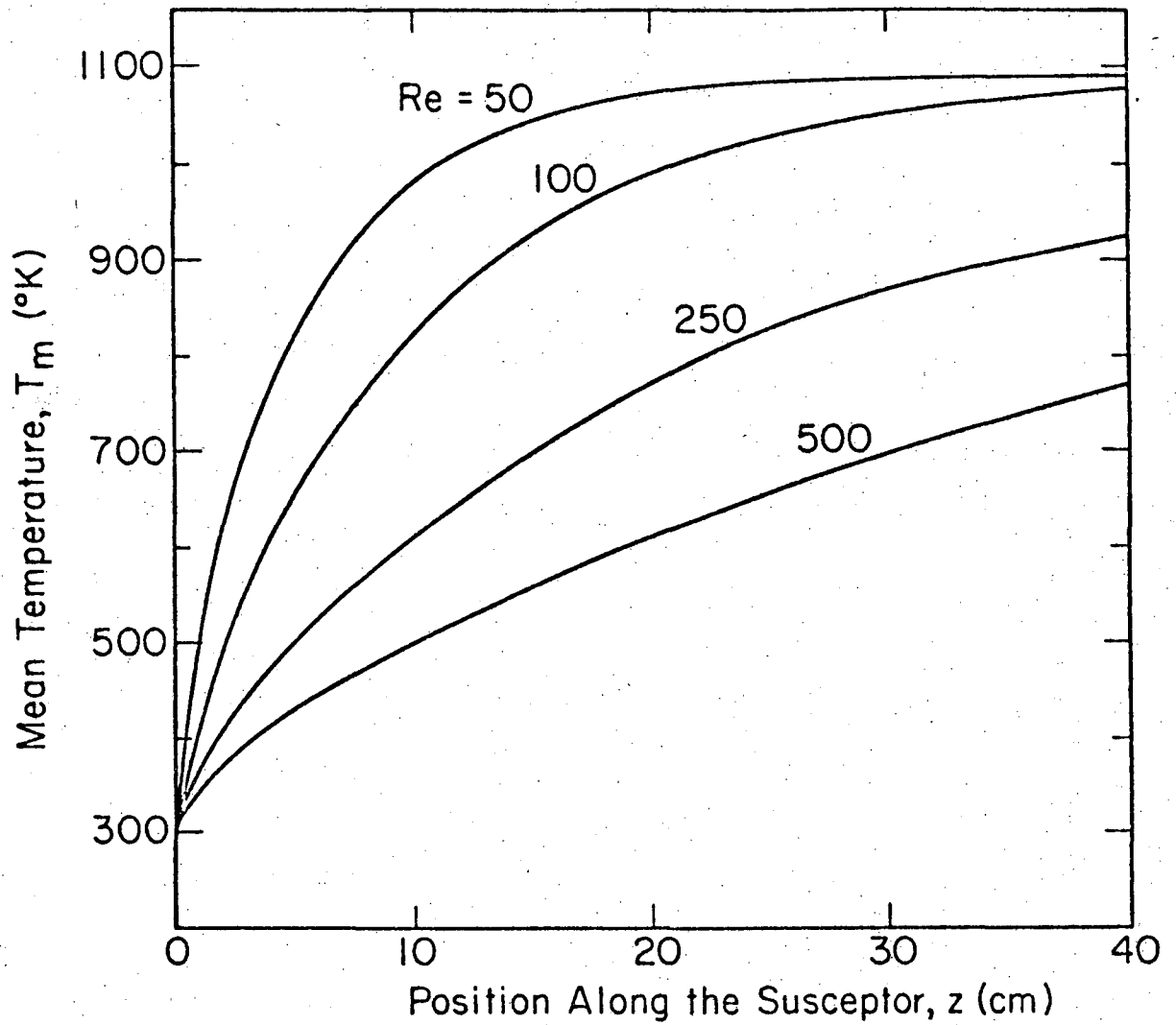
Flow Regime

The range of Reynolds numbers for the operating conditions considered in this study is from 50 to 500. Bird et al. (18) indicate that laminar flow will prevail in annular passages for Reynolds numbers less than 2000. Flow instability in the presence of a large thermal gradient can occur even in laminar flow, however. Curtis and Dismukes (19) and Fuji et al. (5) discuss this possibility and conclude that flow instabilities do not occur for hydrogen rich systems under the conditions for epitaxial silicon deposition.

Temperature Variation Along the Susceptor

Calculation of the mean temperature of the gas from Eq. (13) is described on Appendix III. For average Reynolds Numbers of 50, 100, 250, and 500 at 1 atm, 298°K the results of these calculations are shown in Fig. 2. All of the curves in Fig. 2 show the characteristics of developing heat transfer. In a region of developing heat transfer, the temperature of the gas increases very rapidly with distance near the leading edge. The increase in temperature with distance is more gradual at intermediate distances from the leading edge. At large distances downstream the mean temperature approaches the fully developed value and temperature no longer changes with distance. For the barrel reactor previously described, the fully developed value for the mean temperature is 1088°K. The calculated mean temperature of the gas is less than 90% of the fully developed value along the first 10 cm of the susceptor at $Re = 50$ and the first 20 cm of the susceptor at

-17-



XBL 764-950

FIGURE 2

VARIATION OF THE MEAN TEMPERATURE OF
THE GAS WITH POSITION ALONG THE SUSCEPTOR

$Re = 100$. For Re of 250 and 500, the mean temperature is well below the fully developed value for the entire 40 cm length of the susceptor. As these results indicate, entry region temperature development occurs over a significant portion of the susceptor at Reynolds numbers greater than 50. Since the growth rate is roughly proportional to $T^{0.674}$, the effects of axial temperature variation on growth rate are expected to be large.

Qualitative Effects of Entry Region Temperature Development on Growth Rate

Because of the positive temperature dependence of the growth rate, entry region temperature development can be expected to affect the growth rate in three important ways:

- 1) Overall growth rates will be lower than those predicted by theories which consider temperature to be at the maximum, fully developed value.
- 2) Lower than average temperatures at upstream positions and higher than average temperatures at downstream locations will enhance deposition on the downstream portion of the susceptor, partially compensating for the negative effect of reactant depletion on growth rate. Deposition will therefore be more uniform than predicted by growth rate models which evaluate gas temperature at the fully developed value or a constant length averaged value.
- 3) In spite of the decrease in reactant depletion with increased velocity, the overall growth rate should reach a maximum value as velocity is increased and then decrease with further increases in velocity due to the decrease in average gas temperature. these three

expected results will be discussed further as quantitative growth rate expressions and experimental results are presented.

A Constant Temperature Method for Growth Rate Calculation

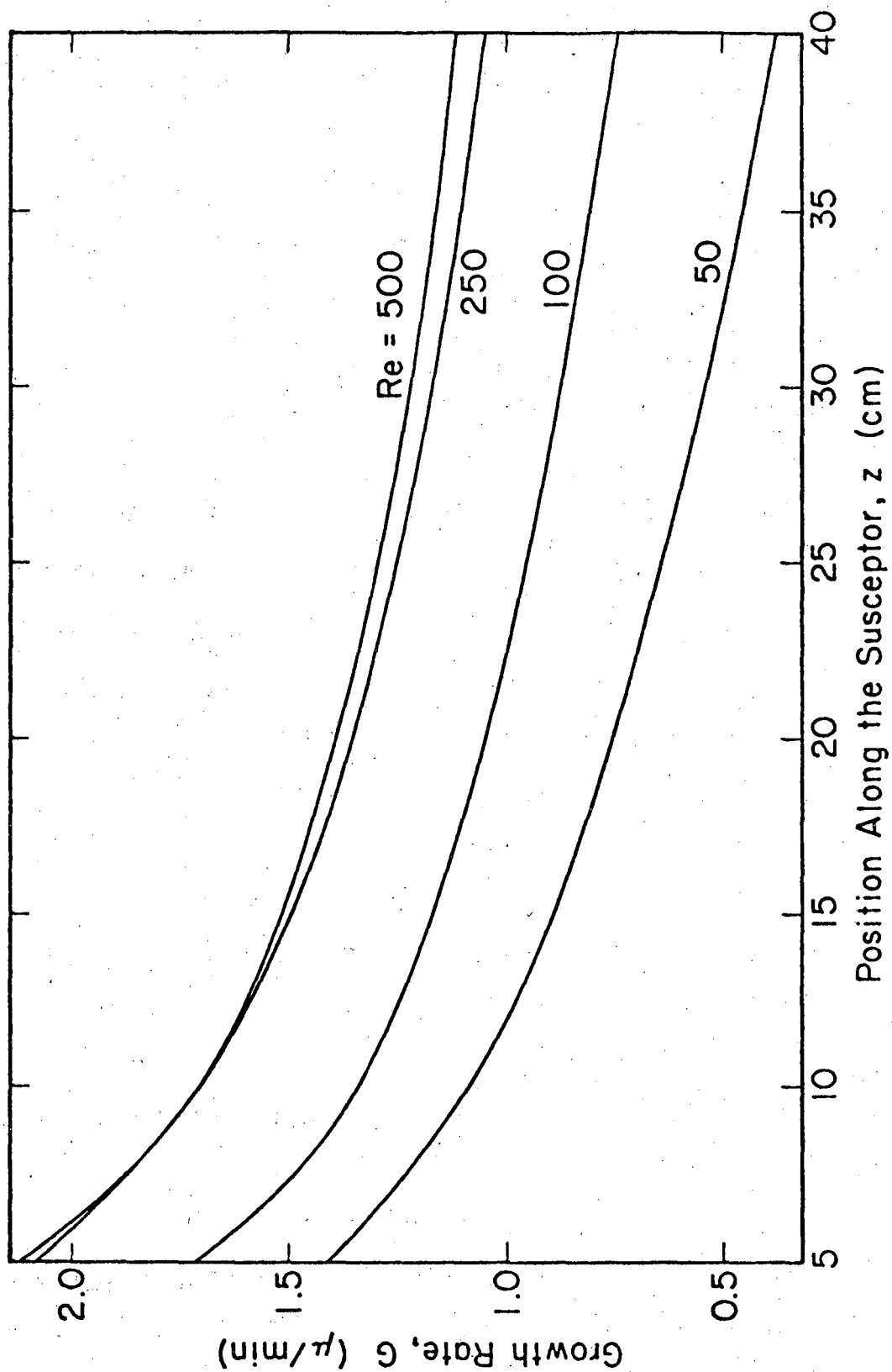
Because of the analogy between heat and mass transfer equations discussed in the theory section, the dimensionless heat transfer solutions of Reynolds et al. (11,12) can be applied directly in the calculation of the growth rate using Eq. (23). With this analogy, developing mass transfer rates in the annular passage are determined subject to the conditions of laminar flow, constant fluid and transport properties, and a fully developed velocity field. Results are shown in Figure 3 for Reynolds Numbers of 50, 100, 250, and 500. High deposition at upstream susceptor positions and low deposition at downstream positions are characteristic of all of the predicted curves. At the lower Reynolds Numbers 50 and 100, the decrease in growth rate with distance is largely a result of reactant depletion. For the higher Reynolds Numbers, however, reactant depletion is a less important factor. Lower resistance to radial diffusion reflected in high values of the Sherwood number in the leading edge flow region results in the prediction of high growth rates for the front portion of the susceptor at the higher velocities. This method considers the effect of developing mass transfer profiles, however, it does not include the effect of simultaneously developing heat transfer in the reactor.

The Developing Temperature Model for Growth Rate Calculation

The heat transfer solutions of Reynolds et al. (11,12) are valid only for constant property flow. Strict application of the solutions to Eq. (23) requires that all parameters be evaluated at a constant

FIGURE 3.

VARIATION OF GROWTH RATE WITH POSITION ALONG A
CONSTANT DIAMETER SUSCEPTOR ACCORDING TO THE
CONSTANT TEMPERATURE MODEL. TRANSPORT PROPERTIES
ARE EVALUATED AT THE AVERAGE MEAN TEMPERATURE OF
THE GAS.



temperature as described above. The heat transfer calculation, however, indicate that temperature will increase with downstream position. An approximate calculation of the growth rate with variable temperature can be made by using Eq. (23) with D_{12} and T_m evaluated at the local T_m of the gas. The basis for this approximation is the assumption that the Sherwood number at a downstream location for flow with changing properties will be nearly equal to the value evaluated at the length average mean temperature. The assumption should be fairly good if the temperature variation in the region of interest along the susceptor is small, but less accurate as temperature variation from the length average value increases. The developing temperature model is therefore expected to work better for low velocities. The accuracy of the method for flow in the barrel reactor at Re of 92.6 is supported by comparison to experimental results which will be presented.

Details of the developing temperature model are given in Appendix II. Results of growth rate calculations are shown in Figure 4. Lower temperatures in the upstream region of the reactor result in calculated growth rates which are lower than those predicted by the constant property method. Deposition in the downstream region is higher because the temperature is greater than the length average value and because the lower predicted values in the upstream portion result in a smaller depletion of the reactant.

A comparison of the developing temperature model to the constant temperature method is shown in Figure 5 for the high and low flow rates. The difference between the two methods is more pronounced for the high

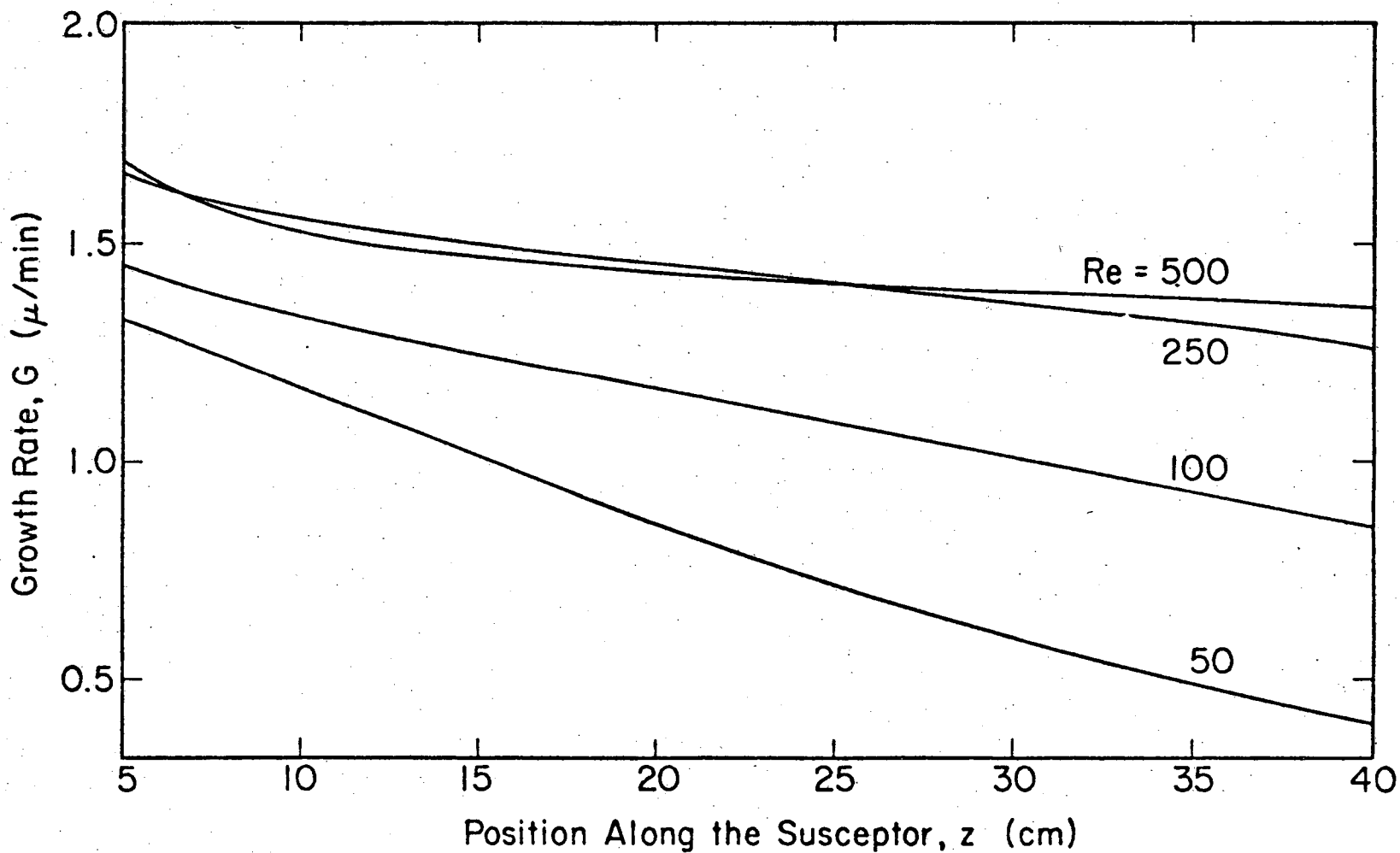
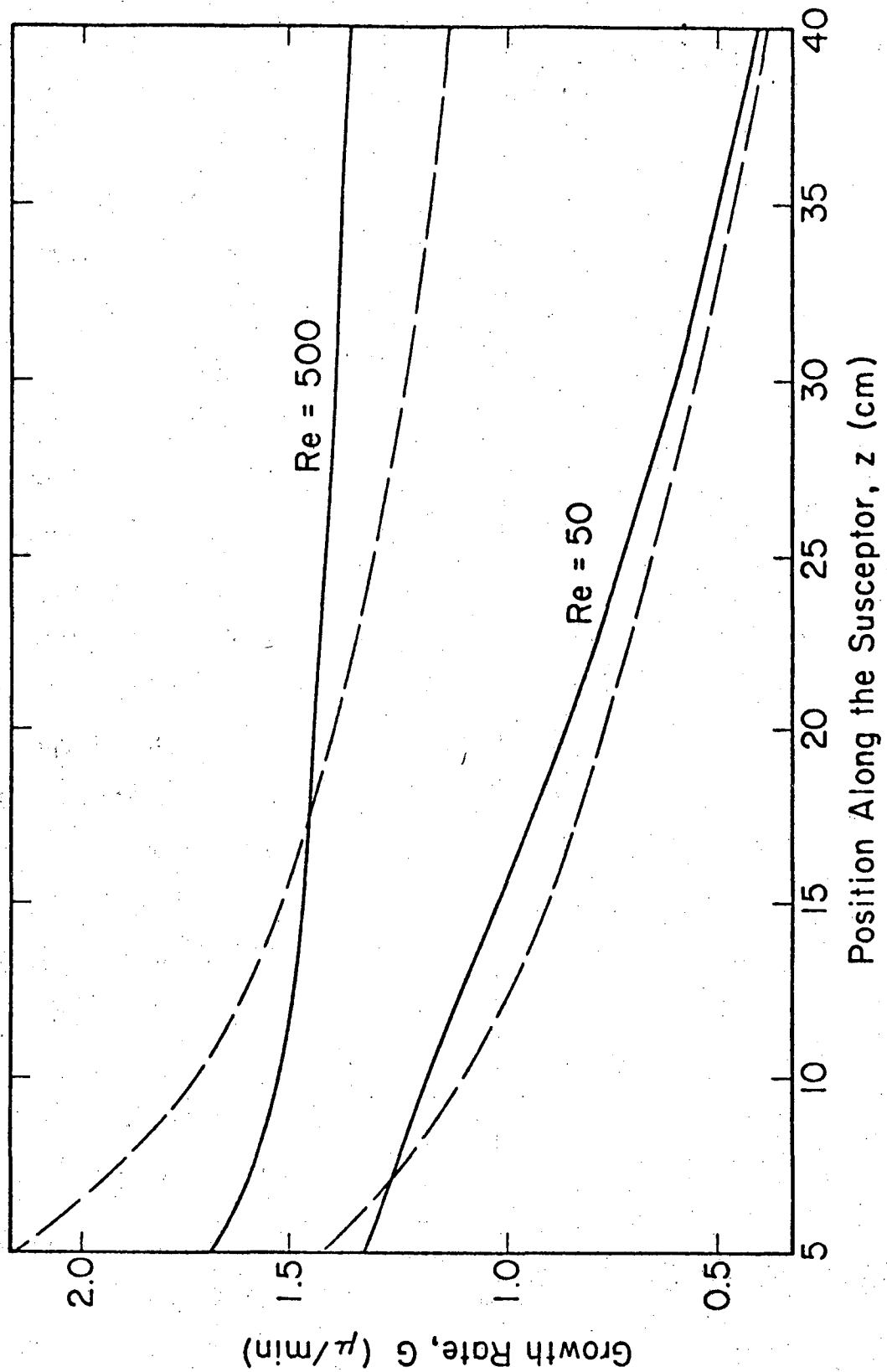


FIGURE 4. VARIATION OF GROWTH RATE WITH POSITION ALONG A CONSTANT DIAMETER SUSCEPTOR ACCORDING TO THE DEVELOPING TEMPERATURE MODEL.

NBL 761-953

FIGURE 5.

COMPARISON OF THE GROWTH RATE VARIATION PREDICTED
BY THE CONSTANT TEMPERATURE MODEL (----) AND THE
DEVELOPING TEMPERATURE MODEL (——).



flow rate since the variation of the local temperature from the length average value is greater. For $Re = 50$, flow is close to being fully developed and the growth rates predicted by the two methods are similar. As expected the variable temperature method predicts a more uniform growth rate distribution than the constant temperature method.

Growth Rates for a Reactor with a Tapered Susceptor

The Sherwood number varies slowly with the parameter, r_i/r_o . If the taper angle is small, the approximate growth rate for a tapered susceptor reactor can be calculated by Eq. (23) using the Sherwood number distribution for the average value of r_i/r_o . Growth rates for a reactor with an average inner diameter of 8.25 cm and a taper angle of 3.58 degrees are presented in Figure 6. Growth rates were calculated by the variable temperature method. Mass transfer to the susceptor is enhanced by the increasing inner radius. For Re of 250 and 500, the result is higher predicted deposition at downstream positions. For Re of 100, enhancement of the growth rate due to the increasing inner radius offsets the effect of reactant depletion and a nearly uniform growth rate distribution is predicted. The constant diameter growth rate is shown for comparison. The Re value of 100 is very close to the design flow for the reactor for which Re is 92.6. At $Re = 50$ the enhancement due to taper angle is insufficient to compensate reactant depletion and the growth rate declines with distance.

Yield, Overall Growth Rate, and Growth Rate Nonuniformity

Table II summarizes yield, overall growth rate, and growth rate nonuniformity predicted by the developing temperature method. Values are calculated for $(5 \leq z \leq 40)$, the approximate useful area of the

FIGURE 6.

VARIATION OF GROWTH RATE WITH POSITION ALONG
A TAPERED SUSCEPTOR (TAPER ANGLE = 3.58°)
ACCORDING TO THE DEVELOPING TEMPERATURE MODEL.

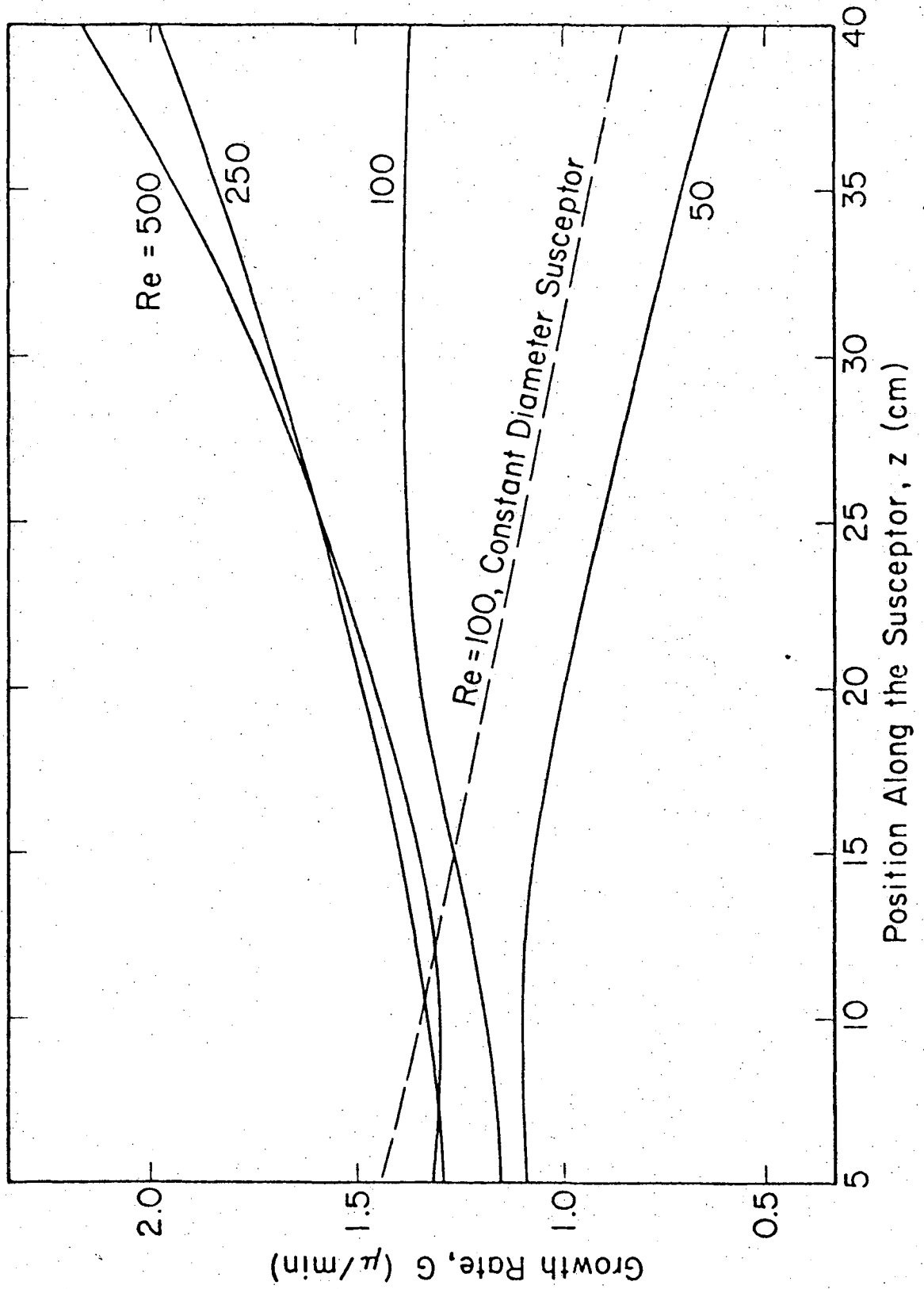


Table II

Yield, overall growth rate, and growth rate non-uniformity.

Constant Diameter Susceptor

<u>Susceptor Dia.</u>	<u>Re₂₉₈</u>	<u>Yield %</u>	<u>$\bar{G}(\mu/\text{min})$</u>	<u>$\Delta G(\%)$</u>
Constant	500	7.42	1.43	10.8
"	250	14.5	1.42	13.2
"	100	29.8	1.13	25.9
"	50	42.7	0.81	53.0

Tapered Susceptor

Tapered 3.58°	100	33.7	1.25	5.9
Tapered 3.58°	92.6	35.5	1.21	4.7

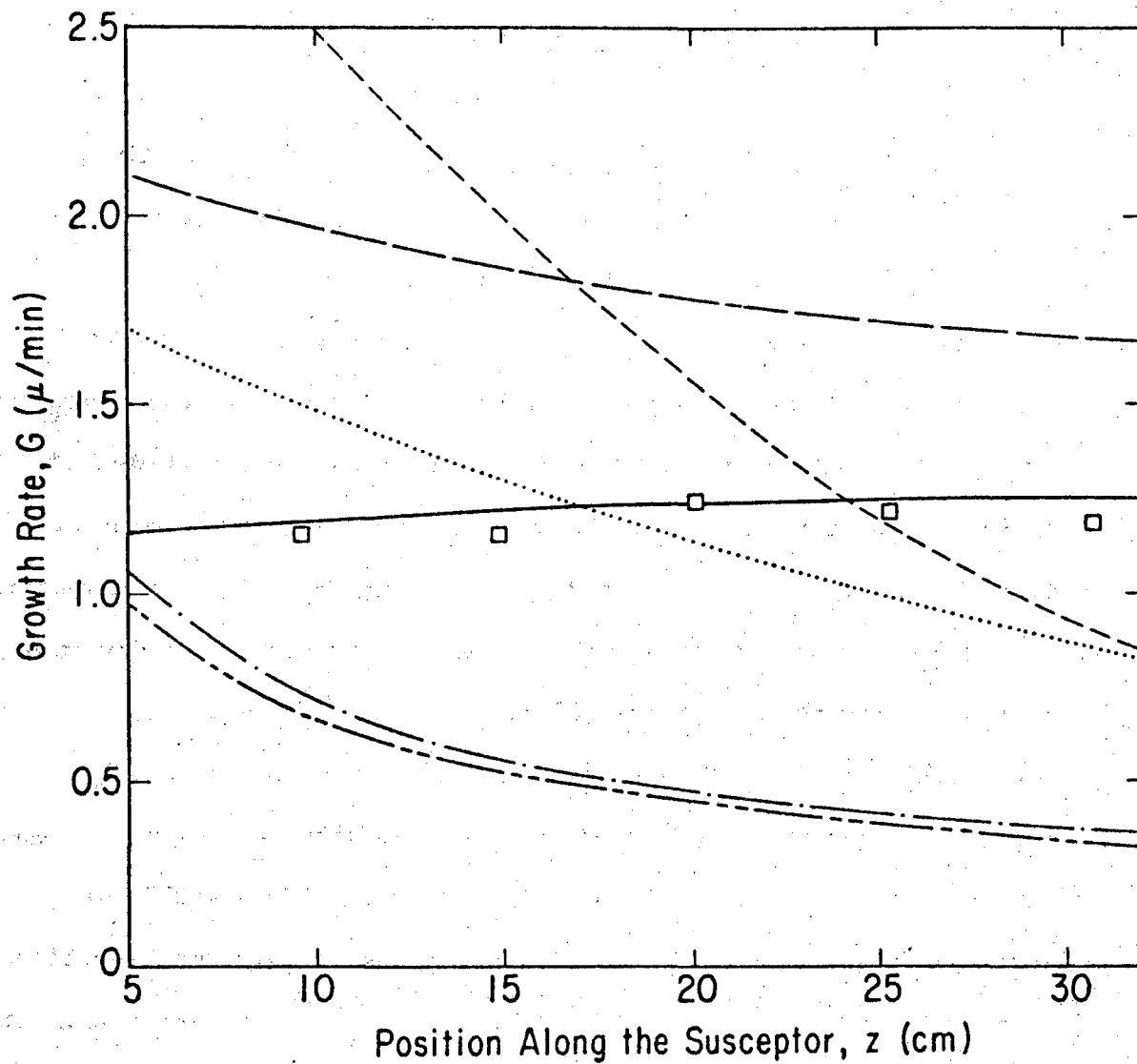
susceptor. Growth rate non-uniformity is evaluated by Eversteyn's method (1):

$$\Delta G = \frac{G_{\max} - G_{\min}}{G_{\max} + G_{\min}} \times 100\% . \quad (26)$$

For a constant diameter susceptor, deposition uniformity is achieved by increasing the flow rate at the expense of reactant yield. Predicted results indicate low growth rate non-uniformity at $Re = 250$ and 500 , but very poor reactant yields. The choice of flow rate for a constant diameter reactor would involve a compromise between the cost of higher reactant throughput at low reactant yield and the cost of reduced finished device yield due to non-uniform deposition. The tapered susceptor reactor offers an attractive alternative to this compromise. Using this innovation, the taper angle may be set to minimize growth rate non-uniformity at a specified velocity. The predicted growth rate non-uniformity for the tapered susceptor reactor at $Re = 100$ is much smaller than for the constant diameter reactor at $Re = 500$. At the design flow $Re = 92.6$, growth rate non-uniformity is further reduced. With the tapered susceptor, predictions indicate that a small growth rate non-uniformity (4.73%) can be attained at an acceptable reactant yield (35.5%).

Comparison to Experimental Results and Other Growth Rate Models

The growth rate predicted by the developing temperature method for a tapered susceptor reactor is compared to the calculations of other models and to experimental values in Figure 7.



XBI 761-952

FIGURE 7.

A COMPARISON OF GROWTH RATE MODELS AND EXPERIMENTAL DATA.
 (—) DEVELOPING TEMPERATURE MODEL, THIS WORK; (---) EVERSTEIJN
 AND PEEK; (— —) FUJII ET AL.; (····) RUNDLE; (— · —) DITTMAN;
 (— -- —) CHILTON-COLBURN ANALOGY. SQUARES ARE EXPERIMENTAL
 DATA.

Experimental data were taken for a commercial barrel reactor, the AMT 740, of the dimensions shown in Fig. 1. The susceptor taper angle is 3.58 degrees. A flow of 112 l/min of 1.15% SiCl_4 - 98.85% H_2 reactant gas was introduced by jets at the top of the reactor, which were adjusted to the optimum setting. Conditions of the experiment are fully described in Chapter Two. Reported Values are wafer center growth rates averaged for the eight susceptor faces. Theoretical predictions are based on a reactor of the same dimensions as the experimental reactor with the same initial SiCl_4 mole fraction at an Re of 9.26 cm/sec corresponding to the 112 l/min flow rate of the experimental reactor. Growth rate is predicted by the developing temperature method for a tapered annulus. Agreement between the theoretical prediction and the experimental data is excellent.

Fujii's model for the growth rate in a barrel reactor with a tapered susceptor predicts values which are higher than observed values, especially for the first 20 cm of the susceptor. This result is expected, as mentioned earlier, because Fujii's growth rate equation is for the fully developed temperature. The fact that Fujii's growth rate equation contains adjustable parameters which were optimized for a barrel reactor of different dimensions may also be partly responsible for the high growth rates. Comparing Fujii's model to the results of this work shows that the developing temperature method of this work is more accurate in both predicting values for the growth rate and representing the variation of growth rate with susceptor position.

Dittman's correlation and the Chilton-Colburn analogy to flow over a flat plate both fail to represent the data quantitatively or qualitatively. Dittman's correlation is based on experimental data taken on a reactor with a very short susceptor and a large separation between the susceptor and reactor wall. Apparently, neither Dittman's correlation nor the Chilton-Colburn analogy to flow over a flat plate provide a realistic description of the growth rate distribution in a reactor of industrial dimensions.

Of the horizontal reactor models, Rundle's method gives growth rates which compare better with the experimental data. Eversteyn's stagnant layer model predicts growth rates which are much higher than observed values for the barrel reactor. Neither author recommends his method for use in predicting growth rates in the vertical reactor.

Of the models examined, the developing temperature method proposed in this work gives the best agreement with the experimental data. It is the only model which predicts the observed lower growth rate values at upstream positions on the susceptor. the developing temperature method incorporates two features not found in the other models studied; it accounts for the effect of increasing temperature on growth rate distribution and it accounts for the reduction in deposition efficiency due to side reaction to SiCl_4 . The excellent agreement between the developing temperature method and the experimental growth rates demonstrates the importance of considering these effect in developing an accurate method for growth rate prediction.

After comparing the results of several models to experimental data, the three predicted effects of developing heat transfer can be

further examined. Experimental growth rates and growth rates predicted by the developing temperature method are both lower than those for Fujii's barrel reactor model in which temperature is considered to be fully developed. This comparison confirms the first prediction; overall growth rates are lower than those predicted for constant, fully developed temperature. Since Fujii's model predicts less uniform growth than either values predicted by the developing temperature method or those observed experimentally, the second expected effect is confirmed. The third expected effect is that the overall growth rate should reach a maximum value and then decrease as the flow rate is increased. The decline in growth rate does not occur in the range of Reynolds Numbers 50 to 500, studied in this paper. Fujii et al. (5), however, have reported experimental results which show that the overall growth rate does decrease at high flow rates.

CONCLUSION

Calculation of heat transfer using the solution by Reynolds et al. (11,12) for developing heat transfer in an annular passage indicates that entry region temperature development will occur over a significant portion of the barrel reactor susceptor at Reynolds numbers greater than 50. Since barrel reactors typically operate at Reynolds numbers close to 100, the assumption of a constant temperature or constant temperature profile throughout the reactor is clearly unsatisfactory.

Due to the positive dependence of the silicon growth rate on mean gas temperature, overall growth rates are expected to be lower than those predicted by models which incorrectly assume the temperature of the gas to be fully developed throughout the reactor. Furthermore, growth rates are expected to be more uniform than predicted by fully developed temperature models. The enhancement of mass transfer rates which accompanies the increase in temperature with downstream position helps to offset the decrease in growth rate caused by reactant depletion. The decline in overall growth rate at very high reactant flow rates observed experimentally by Fujii et al. (5) is also a consequence of developing heat transfer and the positive temperature dependence of growth rate. As the reactant flow rate is increased beyond flow rates for which reactant depletion is significant, the mean temperature of the gas becomes the primary factor influencing growth rate. Further increase in the flow rate results in extension of the entry length for heat transfer and a lower length average mean gas temperature for the reactor, hence a lower overall growth rate.

The developing temperature model for growth rate calculation proposed in this work gives a growth rate temperature dependence of $T^{0.674}$. The developing temperature method predicts growth rates which are in excellent agreement with experimental data obtained for a commercial barrel reactor. The model gives a more satisfactory description of the growth rate in a barrel reactor than any of the previously published models studied. Among the previously published models, Rundle's model for a horizontal reactor seems to give the best comparison to experimental growth rate values. The model based on the Chilton-Colburn analogy to boundary layer flow over a flat plate gave a particularly poor comparison to the experimental growth rates. This comparison confirms that the analogy to flow over a flat plate is an unsatisfactory representation of the geometry and boundary conditions for mass transfer in a barrel reactor of commercial dimensions.

The developing temperature model was used to study the effects of reactant flow rate and susceptor tilt angle on growth rate uniformity and reactant yield. For reactors with non-tapered susceptors it was found that high reactant flow rates would be required to obtain growth rate non-uniformity of ten percent or less. With the susceptor tilted slightly to an angle of 3.58 degrees, however, an optimum growth rate non-uniformity of about five percent could be achieved at a much lower reactant flow rate. Reactant yield was found to drop off sharply with increased flow rate; therefore the overall performance of the tapered susceptor reactor is predicted to be far superior to that of

the non-tapered reactor. This exercise demonstrates the usefulness of the developing temperature model in evaluating process design alternatives in addition to giving the specific result described above. Hopefully this work will be useful as a process design tool as well as contributing to the understanding of transport in the barrel reactor.

REFERENCES

1. F. C. Eversteyn, P. J. W. Severin, C. H. J. v. d. Brekel, and H. L. Peek, J. Electrochem. Soc., 117, 7, 925 (1970).
2. F. C. Eversteyn, and H. L. Peek, Philips Res. Repts., 25, 472 (1970).
3. P. C. Rundle, Intern. J. Electronics, 24, 405 (1968).
4. P. C. Rundle, Journal of Crystal Growth, 11, 6 (1971).
5. E. Fujii, H. Nakamura, K. Haruna, and Y. Koga, J. Electrochem. Soc., 119, 1106 (1972).
6. F. W. Dittman, Chemical Reaction Engineering II, H. M. Hulburt, ed., Advances in Chemistry Series 133, American Chemical Society Washington, D.C. 1974, pp. 463-473.
7. L. Graetz, Am. Phys. Lpz., 18, 79 (1883); 25, 337 (1885).
8. W. Nusselt, Z. Ver Dtsch. Ing. 67, 206 (1923).
9. G. M. Brown, J. AIChE, 6, 179 (1961).
10. A. P. Hatton, A. Quarmby, Int. J. Heat Mass Transfer, 5, 973 (1962).
11. W. C. Reynolds, R. E. Lundberg, and P. A. McCuen, Int. J. Heat Mass Transfer, 6, 483 (1963).
12. R. E. Lundberg, P. A. McCuen, and W. C. Reynolds, Int. J. Heat Mass Transfer, 6, 495 (1963).
13. D. W. Shaw, in Crystal Growth, Theory and Techniques, Vol. 1, C. H. L. Gordon, ed., pp. 1-48, Plenum Press, London-New York, 1974.
14. V. J. Berry and C. R. dePrima, J. Appl. Phys., 23, 195 (1952).
15. R. Rosler, Private Communication, Applied Materials, Inc., Santa Clara, CA.
16. E. Sirtl, L. P. Hunt, and D. H. Sawyer, J. Electrochem. Soc., 121, 919 (1974).

17. R. C. Reid, and T. K. Sherwood, The Properties of Gases and Liquids, 2nd Ed., McGraw-Hill, New York, 1966.
18. R. B. Bird, W. E. Stewart, E. N. Lightfoot, Transport Phenomena, John Wiley & Sons Inc., New York, 1960.
19. B. J. Curtis, and J. P. Dismukes, Journal of Crystal Growth, 17, 128 (1972).

NOMENCLATURE

B	$B = [(r_i/r_o)^2 - 1]/\ln (r_i/r_o)$
D_{12}	diffusion coefficient, cm^2/s
d_h	hydraulic diameter; $d_h = 2(r_o - r_i)$, cm
gz	gravitational constant, 980 cm/s^2
G	linear growth rate, μ/min
\bar{G}	average linear growth rate, μ/min
ΔG	growth rate non-uniformity, %
M	$M = 1 + (r_i/r_o)^2 - B$
M_{si}	molecular weight of silicon, 28 g/mole
\dot{M}	total molar flow rate, mole/s
Nu	Nusselt number, $Nu = \frac{h d_h}{k}$
P	pressure, atm
Pr	prundle number, $Pr = C_p \mu / k$
\bar{r}	$\bar{r} = r/r_o$
r	radial distance, cm
r_i	inner radius, cm
r_o	outer radius, cm
R	gas constant, $R = 82.06 \text{ atm-cm}^3/\text{g-mole}^\circ\text{K}$
Re	Reynolds number, $Re = \frac{\rho d_h v}{\mu}$
Sc	Schmidt number, $Sc = \frac{\mu}{\rho D_{12}}$
Sh	Sherwood number, $Sh = \frac{k_x d_h}{D_{12}} \frac{P}{RT}$
T	temperature, $^\circ\text{K}$
T_i	inner wall temperature, $^\circ\text{K}$
T_o	outer wall temperature, $^\circ\text{K}$

-41-

T_e	entrance temperature, °K
$T_m, T_m(x)$	mean temperature, °K
$U, U(r)$	velocity, cm/s
U_m	mean velocity, cm/s
v	velocity, cm/s
v_r	component of velocity in radial direction, cm/s
v_z	component of velocity in axial direction, cm/s
x	axial distance, cm
\bar{x}	$\bar{x} = \frac{x}{d_h RePr}$
X	mole fraction $SiCl_4$
\bar{X}	mean mole fraction $SiCl_4$
X_i	mole fraction $SiCl_4$ at inner radius
X_e	initial mole fraction $SiCl_4$
z	axial distance, cm
\bar{z}	$\bar{z} = \frac{z}{d_h ReSc}$
α	thermal diffusivity = $k/\rho C_p$
θ	dimensionless temperature
θ_{mi}, θ_{mo}	dimensionless mean temperature functions
μ	absolute viscosity, poise
χ	dimensionless concentration
ρ	density, g/cm ³
ρ_{si}	density of silicon, 2.33 g/cm ³
Ω_o	collision integral

APPENDIX II

TRANSPORT PROPERTIES

VISCOSITY

PURE H₂

The viscosity of pure H₂ is calculated by the equation of Maitland and Smith (1):

$$\ln(\mu/S) = A \ln(T) + B/T + C/T^2 + D \quad (1)$$

where:

$$\begin{aligned} A &= 0.68720 \\ B &= -0.61732 \\ C &= -111.49 \\ D &= -3.9001 \\ S &= 88.0 \end{aligned}$$

μ is given in μ poise

PURE SiCl₄

Viscosity of pure SiCl₄ is given by the corresponding state method of Stiel and Thodos (2,3,4)

$$\mu \xi = (34.0)(10^{-1}) T_r^{0.94} \quad T_r \leq 1.5 \quad (2)$$

$$\mu \xi = (17.78)(10^{-1})(4.58 T_r - 1.67)^{5/8} \quad T_r > 1.5 \quad (3)$$

where:

$$\begin{aligned} \xi &= T_c^{1/6} / M^{1/2} P_c^{2/3} \\ T_r &= T/T_c \\ T_c &= \text{critical temp.} = 506^\circ \text{K} \\ P_c &= \text{critical press.} = 37.1 \text{ atm} \\ M &= \text{molecular wt.} = 169.9 \\ \mu &= \text{viscosity, } \mu \text{ poise} \end{aligned}$$

PURE HCl

Experimental values for the viscosity of pure HCl for temperatures between 298°K and 700°K were correlated to the following equation by least squares linear regression analysis:

$$\mu = \frac{18.794 T^{1.5}}{(367.21 + T)} \quad (4)$$

where μ is given in μ poise. For temperatures above 700°K, viscosity is extrapolated according to the approximate temperature dependence of the Stockmayer potential collision integral in the high temperature range:

$$\mu = 2.7827 T^{0.7272} \quad (5)$$

μ is given in μ poise.

MIXTURE VISCOSITY

The viscosity of the gas mixture is calculated by Wilke's method (5)

$$\mu_{\text{MIX}} = \sum_{i=1}^n \mu_i / \left[1 + \sum_{\substack{j=1 \\ j \neq i}}^n \phi_{ij} (y_j/y_i) \right] \quad (6)$$

where:

$$\phi_{ij} = \left[1 + (\mu_i/\mu_j)^{1/2} (M_j/M_i)^{1/4} \right]^2 / (8 + 8M_i/M_j)^{1/2}$$

μ_i = viscosity of i

y_i = mole fraction of i

M_i = mol.wt. of i

DENSITY OF MIXTURE

The density of the mixture is calculated according to the ideal gas law:

$$\rho_{\text{MIX}} = \frac{P}{RT} \sum_{i=1}^n Y_i M_i \quad (7)$$

HEAT CAPACITY

Heat capacity data for each of the components is given in Ref. (6).

These data were fit to a quadratic form:

$$C_p = A + BT + CT^2 \quad (8)$$

Constants for Eq. (8) are as follows:

$$\begin{aligned} \text{for } H_2, \quad A &= 14534 \\ B &= -0.4023 \\ C &= 9.816 (10^{-4}) \end{aligned}$$

$$\begin{aligned} \text{for } SiCl_4, \quad A &= 561.4 \\ B &= 6.417 (10^{-2}) \\ C &= -8.640 (10^{-6}) \end{aligned}$$

$$\begin{aligned} \text{for } HCl, \quad A &= 774.61 \\ B &= 45.35 (10^{-3}) \\ C &= 45.81 (10^{-6}) \end{aligned}$$

Heat capacity is given in units of joule/Kg-°K.

The heat capacity of the mixture is determined by adding the component heat capacities weighted according to mole fractions:

$$C_{PMIX} = \sum_{i=1}^n C_{p_i} \left(\frac{Y_i M_i}{M_{MIX}} \right) \quad (9)$$

THERMAL CONDUCTIVITY

PURE H_2

Experimental data from the literature has been fit to the following second order polynomial:

$$k = .080796 + 3.7312 (10^{-4})T - 7.4683 (10^{-9})T^2 \quad (10)$$

k is given in joule/(M sec °K)

PURE $SiCl_4$

Euken's method (7) is used to relate thermal conductivity to viscosity:

$$k = C_{p_{SiCl_4}} + 61.18 \mu_{SiCl_4} \quad (11)$$

k is given in joule/(M sec °K).

PURE HCl

For temperatures below 700°K, data from the literature is correlated by:

$$k = 2.104 (10^{-3}) + 3.676 (10^{-5}) T + 1.462 (10^{-8}) T^2 \quad (12)$$

joules/(M sec °K)

for temperatures greater than 700°K, thermal conductivity is calculated by the Eucken Method (7)

$$k = .9661 (Cp_{HCl} + 285.1) \mu_{HCl} \quad (13)$$

MIXTURE THERMAL CONDUCTIVITY

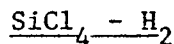
The mixture thermal conductivity is calculated by the Mason and Saxena (8) formulation of the Wassiljewa Equation:

$$k_{mix} = \sum_{i=1}^n k_i / \left[1 + \sum_{j=1}^n A_{ij} (Y_j/Y_i) \right] \quad (14)$$

The parameter A_{ij} may be taken as equal to the parameter ϕ_{ij} used on Wilke's equation (6) for the mixture viscosity.

BINARY DIFFUSION COEFFICIENTS

Binary diffusion coefficients were estimated using the theoretical equation (7).



Using the combined potential parameters:

$$\sigma_{12} = 4.31 \text{ \AA}$$

$$\frac{\epsilon_{12}}{k} = 144^\circ \text{K}$$

the theoretical equation gives

$$D_{\text{SiCl}_4 - \text{H}_2} = 7.0861 (10^{-9}) T^{3/2} / \Omega_D \quad \text{m}^2/\text{sec} \quad (15)$$

HCl - H₂

Using $\sigma_{12} = 3.083 \text{ \AA}$ and $\epsilon_{12}/k = 143^\circ \text{K}$, the theoretical equation

is:

$$D_{\text{HCl-H}_2} = 1.4196 (10^{-8}) T^{3/2} / \Omega_D \quad \text{M}^2/\text{sec} \quad (16)$$

Ω_D may be evaluated from tabulated values or by

$$\Omega_D = \frac{A}{BT^*} + \frac{C}{\exp(DT^*)} + \frac{E}{\exp(FT^*)} + \frac{G}{\exp(HT^*)} \quad (17)$$

$$T^* = \frac{kT}{\epsilon_{12}}$$

$$A = 1.06036$$

$$F = 1.52996$$

$$B = 0.15610$$

$$G = 1.76474$$

$$C = 0.1930$$

$$H = 3.89411$$

$$D = 0.47635$$

$$E = 1.03587$$

REDUCED TRANSPORT PARAMETERS

Reynolds Number:

$$Re_{\text{mix}} = \frac{\rho_{\text{mix}} d h v}{\mu_{\text{mix}}}$$

Prandtl Number:

$$Pr_{\text{mix}} = \frac{C_{p\text{mix}}}{\frac{(\mu_{\text{mix}})}{k_{\text{mix}}}} \mu_{\text{mix}}$$

Schmidt Number for SiCl₄ - H₂:

$$Sc_{\text{SiCl}_4 - \text{H}_2} = \frac{\mu_{\text{mix}}}{\rho_{\text{mix}} D_{\text{SiCl}_4 - \text{H}_2}}$$

Schmidt Number for HCl - H₂:

$$Sc_{\text{HCl} - \text{H}_2} = \frac{\mu_{\text{mix}}}{\rho_{\text{mix}} D_{\text{HCl} - \text{H}_2}}$$

REFERENCES

1. G.C. Maitland and E.B. Smith, J. Chem. and Engineering Data, 17:2 (1972).
2. L.I. Stiel and G. Thodos, AIChE J., 7:611, (1961).
3. L.I. Stiel and G. Thodos, AIChE J., 10:266, (1964).
4. L.I. Stiel and G. Thodos, "Progress in International Research on Thermodynamics and Transport Properties", Academic Press, New York, 1962, pp. 352-365.
5. C.R. Wilke, J. Chem. Phys., 18:517, (1950).
6. JANAF TABLES
7. R.C. Reid and T.K. Sherwood, "The Properties of Gases and Liquids", 2nd Ed., McGraw Hill Book Co., New York, 1966.
8. E.A. Mason and S.C. Saxena, Phys. Fluids, 1:361, (1958).

LEGAL NOTICE

This report was prepared as an account of work sponsored by the United States Government. Neither the United States nor the United States Energy Research and Development Administration, nor any of their employees, nor any of their contractors, subcontractors, or their employees, makes any warranty, express or implied, or assumes any legal liability or responsibility for the accuracy, completeness or usefulness of any information, apparatus, product or process disclosed, or represents that its use would not infringe privately owned rights.

TECHNICAL INFORMATION DIVISION
LAWRENCE BERKELEY LABORATORY
UNIVERSITY OF CALIFORNIA
BERKELEY, CALIFORNIA 94720